

Magnetization reversal dynamics with submicron-scale coercivity variation in ferromagnetic films

Sug-Bong Choe and Sung-Chul Shin

Department of Physics and Center for Nanospinics of Spintronic Materials, Korea Advanced Institute of Science and Technology, Taejeon 305-701, Korea

(Received 15 June 2000)

We report experimental evidence that submicron-scale local coercivity variation determines magnetization reversal dynamics in ferromagnetic thin films. Local coercivity distribution is generated from a two-dimensional array of hysteresis loops each of $0.32 \times 0.32 \mu\text{m}^2$ spots simultaneously measured using a magneto-optical microscope magnetometer. We directly demonstrate that domain reversal pattern is truly coincident with local coercivity variation. Local switching time of domain evolution is found to be exponentially dependent on local coercivity governed by a thermally activated relaxation process.

Magnetization reversal dynamics in ferromagnetic materials continues to be a fundamental issue in magnetism.^{1,2} Interest has rapidly grown by the recent technological achievement of the magnetoelectronics such as the magnetic disks, tapes, sensors, and memories, which demands the elaborated exploration on the dynamic properties of magnetic materials having the physical and/or chemical microstructures.³⁻⁸ Recently, advanced magnetic imaging techniques provide the direct evidences of the contrasting domain dynamics both for wall-motion dominated and nucleation dominated processes in those magnetic materials.⁹⁻¹²

To clarify the origin of the contrasting reversal dynamics, numerous studies have been carried out under a variety of conditions.⁷⁻¹² Macroscopic magnetic properties have been examined to explain the intrinsic origin of the reversal dynamics by a thermally activated relaxation process based on a micromagnetic description of the sample. It was explained that contrasting reversal dynamics could occur among uniform magnetic films that possess different macroscopic magnetic properties.¹²⁻¹⁴

In addition, structural irregularities have been conjectured to be yet another origin of the contrasting reversal dynamics and magnetic domain structures.^{10,15-19} It is also a very crucial issue in technological achievement as the size of the individual element approaches the size of the structural irregularities.³ It is obvious that the domain evolution is locally affected by the magnetic inhomogeneity,¹⁶ as demonstrated for the "Swiss-cheese" -shaped domains in ferromagnetic Au/Co/Au films with introducing the local coercivity distribution¹⁷ or for the anisotropic domain propagation in the vicinity of the artificially induced miscut step-edge in epitaxial Pt/Co/Pt films.¹⁸ However, all the previous investigations have been done based on the models of the coercivity distribution, and the question on real films remains open.

The fundamental understanding needed to address this question requires microscopic studies, including measurements of the microstructural (or micromagnetic) properties and real-time observation of the evolution of the domain structure in a magnetic field. Most importantly, both experiments need to be carried out on *identical* microscopic areas of the sample. Many experimental techniques of magnetic imaging²⁰⁻²² have been devoted to investigate microscopic

domain structures with spatial resolution of some tens of nanometers. But, despite the high spatial resolution of these techniques, they are not applicable to dynamical studies due to the limitations imposed by applying a magnetic field and/or slow data acquisition times. On the other hand, the quantitative characterization of a submicron-size magnetic dots have been carried out by means of the magneto-optical Kerr effect while either using a focused laser beam^{5,15} or using an optical microscope equipped with a charge-coupled device (CCD) camera.^{6,7} However, to the best of our knowledge, the direct correlation of the local hysteresis loops with the domain dynamics in continuous ferromagnetic films has not been reported yet.

The present study was motivated to clarify the mechanism responsible for how submicron-scale structural irregularities affect the domain reversal dynamics and domain structures. For this study, we have developed a magneto-optical microscope magnetometer (MOMM) capable of local hysteresis loop measurements as well as real-time domain evolution image analysis with submicron spatial resolution.²³ Using the MOMM system, we have monitored structural inhomogeneity via the measurement of local coercivity variations, taking advantage of the fact that coercivity is a structure-sensitive magnetic property.²⁴ The local coercivity distribution is first generated and then, the time-resolved domain patterns during magnetization reversal are taken at *precisely the same* positions. This paper reports experimental observation that magnetization reversal dynamics is directly related to the submicron-scale coercivity variation, which could be quantitatively explained based on a thermally activated relaxation process.

The MOMM system mainly consists of an optical polarizing microscope capable of $1000\times$ magnification with spatial resolution of $0.4 \mu\text{m}$ and Kerr-angle resolution of 0.2° .¹² To measure hysteresis loops, the system is equipped with a computer-controlled electromagnet to sweep the external field in the range of ± 5 kOe. Domain images are captured by a CCD camera system interfaced to the computer. The images are composed of the light intensity distribution measured by the CCD array of 100×80 pixels, where a unit pixel corresponds to the local area of $0.32 \times 0.32 \mu\text{m}^2$ of the film surface. By storing the domain images while sweeping the external field H , it is possible to

generate an array of the local intensity variation $I_{xy}(H)$ as a function of H . This is done by tracing the intensity variation at every corresponding (x,y) th CCD pixels. Then, the normalized Kerr hysteresis loop $\theta_{xy}(H)$ can be obtained by fitting the measured $I_{xy}(H)$ for the two saturated states.²³ It should be emphasized that the Kerr hysteresis loop is obtained for each CCD pixel and thus, 8000 Kerr hysteresis loops can be simultaneously obtained. We generate a map of the local coercivity distribution $H_C(x,y)$ by measuring the coercivity from every corresponding hysteresis loop for each CCD pixel at (x,y) , where every hysteresis loop is measured under the identical condition at room temperature at a fixed field sweeping rate. The local coercivity distribution $H_C(x,y)$ is further deconvoluted by $H_C(x,y) = H_C^0 + \delta H_C(x,y)$, where H_C^0 is the mean value of the local coercivity and $\delta H_C(x,y)$ is the local coercivity variation.

We have used the apparatus to investigate the Co/Pd multilayered system, where the reversal dynamics were reported to sensitively change from being dominated by wall motion to being nucleation dominated by increasing either the number of repeats¹¹ or the Co-layer thickness.¹² The contrasting reversal behavior with changing the Co-sublayer thickness was revealed to be mainly caused by the change in the strength of the demagnetizing field.¹² In the present study, we focus on the reversal phenomena by varying the numbers of repeats, where the structural irregularity is expected to increase due to the possible accumulation of the lattice misfits, residual stress, and other defects at the number of interfaces during deposition process in high vacuum, while the intrinsic magnetic properties are basically unchanged. The individual layer thicknesses were kept constant to prevent changes in the macroscopic magnetic properties. Multilayered samples of $(2.5\text{-}\text{\AA} \text{ Co}/11\text{-}\text{\AA} \text{ Pd})_n$ with varying number of repeats n from 5 to 15, were prepared on glass substrates by e-beam evaporation under a base pressure of 2.0×10^{-7} Torr at ambient temperature. The layer thickness was controlled within a 4% accuracy.¹² Low-angle x-ray diffraction studies using Cu $K\alpha$ radiation revealed that all samples had distinct peaks indicating an existence of the multilayer structure. High-angle x-ray diffraction studies showed that the samples grew along the [111] cubic orientation. All the samples have perpendicular magnetic anisotropy and show M - H hysteresis loops of unit squareness.

As expected, the local coercivity variation was found to increase with increasing n . In Fig. 1, we illustrate the coercivity distribution of (a) $n=5$, (b) 10, and (c) 15, respectively, by mapping $\delta H_C(x,y)$ onto the two-dimensional XY plane, where each map corresponds to a sample surface area of $32.0 \times 25.6 \mu\text{m}^2$. Each coercivity distribution was determined by measuring the local hysteresis loops under an identical condition of the sweeping rate of 10 Oe/s for each

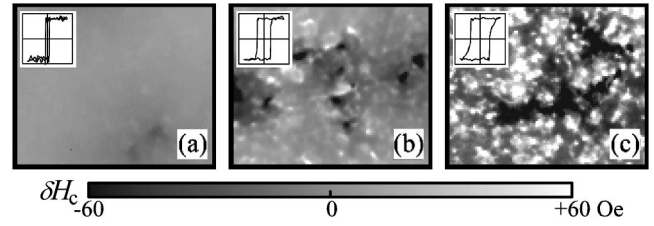


FIG. 1. Local coercivity distributions $\delta H_C(x,y)$ of the $(2.5\text{-}\text{\AA} \text{ Co}/11\text{-}\text{\AA} \text{ Pd})_n$ samples with (a) $n=5$, (b) 10, and (c) 15, respectively, on a sample area of $32.0 \times 25.6 \mu\text{m}^2$. The inset shows the typical hysteresis loop measured at a unit pixel of $0.32 \times 0.32 \mu\text{m}^2$, where x axis is applied field H ranging from -2 to 2 kOe and y axis is the normalized Kerr rotational angle.

sample, respectively. The typical shape of local hysteresis loops of a unit $0.32 \times 0.32 \mu\text{m}^2$ area measured at ambient temperature is illustrated in the inset of each figure. Note that the coercivity distribution changes with increasing n : the thinner film with $n=5$ shows a smoother variation of the coercivity, while the thicker film with $n=15$ shows a larger fluctuation in the coercivity. The standard deviation ΔH_C of the coercivity distribution and the mean coercivity H_C^0 increased with increasing n as listed in Table I. A larger coercivity variation of the thicker film is possibly ascribed to a larger H_C^0 , when the variation mainly occurred by a fluctuation in the coercivity. However, we like to point out that the local coercivity is varied not only in the magnitude but also in the spatial distribution, which evidences a larger density of the microstructural irregularities in the thicker film. AFM studies of these samples indeed revealed a tendency towards larger surface roughness with increasing n .

The local coercivity is determined not only by its intrinsic nature but also by the interaction with the magnetization states of the neighbor regions. For instance, the sample having $n=5$ shows a smooth gradient of the coercivity distribution around the low-coercive nucleation site as seen in Fig. 1(a). This gradient is possibly caused by the domain propagation from the nucleation site while sweeping H , rather than by the smooth change in the intrinsic magnetic properties, since this gradient is predicted even for a uniform region in the vicinity of a nucleation site with a finite sweeping rate at a finite temperature. The coercivity gradient is inherently reproduceable in a given sample and it cannot be noticeably modified without breaking the sample.

Magnetization reversal dynamics of the Co/Pd multilayers were investigated via time-resolved observation of domain evolution by applying a constant reversing magnetic field of about 90% of H_C^0 , starting from the saturated state.¹² The reversal phenomenon in this system was found to sensitively change from wall-motion dominant to nucleation dominant

TABLE I. Experimentally determined values of the magnetic parameters of the $(2.5\text{-}\text{\AA} \text{ Co}/11\text{-}\text{\AA} \text{ Pd})_n$ multilayers.

n	H_C^0 (Oe)	ΔH_C (Oe)	M_S (emu/cm ³)	α	β (kOe ⁻¹)	V_A (10 ⁻¹⁸ cm ³)
5	149	6	289	5.3±0.9	111±4	16.0±0.6
10	638	19	333	4.9±1.2	63±5	7.9±0.7
15	916	45	357	3.9±1.8	30±9	3.5±1.0

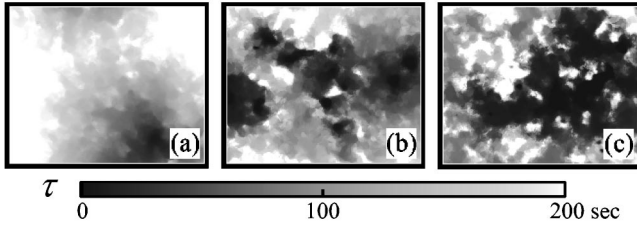


FIG. 2. Local switching time $\tau(x,y)$ determined from the time-resolved domain reversal patterns of the $(2.5\text{-}\text{\AA}\text{ Co}/11\text{-}\text{\AA}\text{ Pd})_n$ samples with (a) $n=5$, (b) 10, and (c) 15, respectively, at exactly the same positions of the corresponding samples shown in Fig. 1.

with increasing n .¹¹ Figure 2 shows the time-resolved domain evolution during magnetization reversal for samples of (a) $n=5$, (b) 10, and (c) 15, respectively, where the color corresponds to the local switching time $\tau(x,y)$ of the corresponding region (x,y) . The domain patterns of the samples were grabbed at *precisely the same* position of each sample shown in Fig. 1. The reversal experiments were carried out 16 times repeatedly for a given sample, since the reversal phenomenon is inherently governed by statistical switching probability. Wall-motion dominant reversal is vividly seen in the sample of $n=5$, while nucleation dominant reversal is clearly observed in the sample of $n=15$. These contrasting reversal patterns occur due to a counterbalance between the nucleation process and the wall-motion process.¹⁰ Smooth variation of domain reversal pattern in Fig. 2(a) indicates a gradual expansion of domains via the continuous wall-motion process from a single nucleation site, while the disorderly dendritic pattern in Fig. 2(c) manifests an anisotropic jutting out of domain sprouts adjacent to the existing domain boundary via the nucleation process.¹²

Most importantly, these contrasting reversal patterns are truly coincident with the coercivity distributions of the corresponding samples. This directly demonstrates the close correlation between the coercivity distribution and domain reversal pattern on the submicron scale. For a quantitative analysis of the correlation, we have measured the number of pixels $N(\delta H_C, \tau)$ obtained by counting the pixels having the corresponding values of $\delta H_C(x,y)$ and $\tau(x,y)$ measured at the same (x,y) th pixel in each map. Figure 3 illustrates the correlated distribution of $N(\delta H_C, \tau)$ in logarithmic scale in the δH_C - τ coordinate. In the figures, we again see that the local switching time is truly correlated with the coercivity distribution. It is interesting to note that the correlated distribution is very definite in the thinner sample, while it is rather diffused in the thicker sample. These results are understandable because the former sample has only a few nucleation site and thus, the reversal is always initiated at the nucleation site followed by the successive wall-motion process at every domain boundary, even though the minor deflection randomly occurs by the thermal fluctuation for a number of observations. On the other hand, the latter sample has a lot of nucleation sites and thus, the reversal is initiated at one of them proceeded by the others, since the nucleation itself is randomly selected by the statistics based on the nucleation probability. It was experimentally confirmed that by averaging over a larger number of observations the reversal pattern approached a certain statistical ensemble.

A fundamental question is whether the local switching

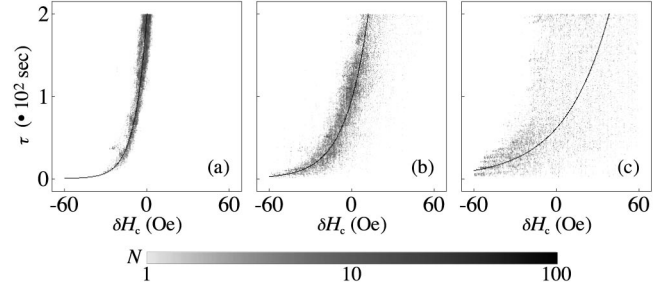


FIG. 3. Correlated distribution of the number of pixels $N(\delta H_C, \tau)$ of the $(2.5\text{-}\text{\AA}\text{ Co}/11\text{-}\text{\AA}\text{ Pd})_n$ samples with (a) $n=5$, (b) 10, and (c) 15, respectively, in logarithmic gray level onto the δH_C - τ coordinate. The solid line in each figure represents the best fit by a function of $\log \tau = \alpha + \beta \cdot \delta H_C$.

time is governed by a thermally activated relaxation process dependent on the local coercivity distribution. Each solid line in Fig. 3 exhibits the best fit of the correlated distribution by a fitting function of

$$\ln \tau = \alpha + \beta \cdot \delta H_C, \quad (1)$$

where α and β are the fitting parameters. The values of α and β are listed in Table I. The exponential dependency could be analyzed within the context of a thermally activated relaxation process. The half reversal time, the time needed to reverse half the volume of the sample, is known to be exponentially dependent on an applied field H .²⁵ By considering the distribution $H_C(x,y)$, the local switching time $\tau(x,y)$ of the magnetization M_S of a volume V_A located at (x,y) is given by

$$\tau(x,y) = \tau_0 \exp\left(\frac{V_A M_S}{k_B T} [H_C(x,y) - H]\right), \quad (2)$$

where τ_0 is the characteristic switching time when $H = H_C(x,y)$ under a finite temperature T .¹⁰ The equation is derived from the Néel-Brown model under an assumption of the first-order uniaxial anisotropy by linear expansion of the energy barrier with H near H_C^0 . Equation (2) is identical to the fitting function of Eq. (1) when $\alpha \equiv \ln \tau_0 + V_A M_S (H_C^0 - H)/k_B T$ and $\beta \equiv V_A M_S / k_B T$. Note that the activation volume V_A can be determined from the experimental values of M_S and the fitting parameter β . The activation volumes of the Co/Pd multilayers were found to be decreased from 1.6×10^{-17} to 3.5×10^{-18} cm^3 with increasing n as listed in Table I. These results are almost identical to the values of our previous approach,²⁶ where the activation volume was experimentally measured from the field dependence of the half reversal time in the whole area of the sample.

In conclusion, we demonstrate a direct relation between the local coercivity variation and the local switching time by experimental measurement of local hysteresis loops as well as real-time domain evolution images with submicron spatial resolution. The local switching time was found to be exponentially dependent on the local coercivity variation and it

could be quantitatively explained based on a thermally activated relaxation process. Thus, the contrasting magnetization reversal dynamics could be understood as being controlled by the degree of local coercivity variation in the presence of structural irregularities.

The authors would like to thank S. Bader, D. Dahlberg, J. Ferré, and B. Raquet for discussions and their critical readings of the manuscript. This work was supported by the Creative Research Initiatives of the Ministry of Science and Technology of Korea.

-
- ¹G. Bertotti, *Hysteresis in Magnetism* (Academic Press, San Diego, 1998), Part IV.
- ²A. Hubert and R. Schäfer, *Magnetic Domains* (Springer-Verlag, Berlin, 1998), Part 6.
- ³J.L. Simonds, *Phys. Today* **48** (4), 26 (1995) and references therein.
- ⁴S. Gider, B.-U. Runge, A.C. Marley, and S.S.P. Parkin, *Science* **281**, 797 (1998).
- ⁵R.P. Cowburn, D.K. Koltsov, A.O. Adeyeye, and M.E. Welland, *Appl. Phys. Lett.* **73**, 3947 (1998); R.P. Cowburn, A.O. Adeyeye, and M.E. Welland, *Phys. Rev. Lett.* **81**, 5414 (1998).
- ⁶T. Aign, P. Meyer, S. Lemerle, J.P. Jamet, J. Ferré, V. Mathet, C. Chappert, J. Gierak, C. Vieu, F. Rousseaux, H. Launios, and H. Bernas, *Phys. Rev. Lett.* **81**, 5656 (1998).
- ⁷J.-P. Jamet, S. Lemerle, P. Meyer, J. Ferré, B. Bartenlian, N. Bardou, C. Chappert, P. Veillet, F. Rousseaux, D. Decanini, and H. Launois, *Phys. Rev. B* **57**, 14 320 (1998).
- ⁸B. Raquet, R. Mamy, and J.C. Ousset, *Phys. Rev. B* **54**, 4128 (1996).
- ⁹J. Ferré, J.P. Jamet, and P. Meyer, *Phys. Status Solidi A* **175**, 213 (1999).
- ¹⁰J. Pommier, P. Meyer, G. Penissard, J. Ferré, P. Bruno, and D. Renard, *Phys. Rev. Lett.* **65**, 2054 (1990).
- ¹¹S.-B. Choe and S.-C. Shin, *J. Appl. Phys.* **85**, 5651 (1999).
- ¹²S.-B. Choe and S.-C. Shin, *Phys. Rev. B* **57**, 1085 (1998); *Appl. Phys. Lett.* **70**, 3612 (1997).
- ¹³R.D. Kirby, J.X. Shen, R.J. Hardy, and D.J. Sellmyer, *Phys. Rev. B* **49**, 10 810 (1994).
- ¹⁴A. Lyberatos, J. Earl, and R.W. Chantrell, *Phys. Rev. B* **53**, 5493 (1996).
- ¹⁵H.-P.D. Shieh and M.H. Kryder, *IEEE Trans. Magn.* **24**, 2464 (1988).
- ¹⁶P. Bruno, G. Bayreuther, P. Beauvillain, C. Chappert, G. Lugert, D. Renard, J.P. Renard, and J. Seiden, *J. Appl. Phys.* **68**, 5759 (1990).
- ¹⁷J. Ferré, V. Grolier, P. Meyer, S. Lemerle, A. Maziewski, E. Stefanowicz, S.V. Tarasenko, V.V. Tarasenko, M. Kisielewski, and D. Renard, *Phys. Rev. B* **55**, 15 092 (1997).
- ¹⁸P. Haibach, M. Huth, and H. Adrian, *Phys. Rev. Lett.* **84**, 1312 (2000).
- ¹⁹M. Speckmann, H.P. Oepen, and H. Ibach, *Phys. Rev. Lett.* **75**, 2035 (1995).
- ²⁰E. Dan Dahlberg and J.-G. Zhu, *Phys. Today* **48** (4), 34 (1995) and references therein.
- ²¹H. Poppa, E. Bauer, and H. Pinkvos, *MRS Bull.* **20**, 38 (1995).
- ²²R. Wiesendanger, H.-J. Güntherodt, G. Güntherodt, R.J. Gambino, and R. Ruf, *Phys. Rev. Lett.* **65**, 247 (1990).
- ²³S.-B. Choe and S.-C. Shin, *J. Appl. Phys.* **87**, 6848 (2000).
- ²⁴H. Kronmüller, *Phys. Status Solidi B* **144**, 385 (1987).
- ²⁵M. Labrune, S. Andrieu, F. Rio, and P. Bernstein, *J. Magn. Magn. Mater.* **80**, 211 (1989).
- ²⁶S.-B. Choe and S.-C. Shin, *J. Appl. Phys.* **87**, 5076 (2000).